J. Astrophys. Astr. (1999) **20**, 51–65

Density and Temperature Diagnostics of Solar Emission Lines from NeV/MgV and SiVII/MgVII Ions

Anita Mohan & B.N. Dwivedi, *Department of Applied Physics, Institute of Technology, Banaras Hindu University, Varanasi 221 005, India.*

P. K. Raju, *Indian Institute of Astrophysics, Bangalore 560 034, India.*

Received 1998 June 5; accepted 1999 June 2

Abstract. We present NeV/MgV and SiVII/MgVII theoretical line intensity ratios as a function of electron density N_e and temperature T_e . These are shown in the form of ratio-ratio diagrams, which should in principle allow both N_e and T_e to be deduced for the emitting region of the solar plasma. We apply these diagnostics in the solar atmosphere, and discuss the available observations made from space. In most cases, however, we deduce N_e and T_e from the computed absolute line intensities in a spherically symmetric model atmosphere of the Sun. Possible future applications of this investigation to spectral data from the Coronal Diagnostic Spectrometer (CDS) on the Solar and Heliospheric Observatory (SOHO) are briefly discussed.

Key words. Solar atmosphere—EUV diagnostics—emission lines—spectroscopic diagnostics.

1. Introduction

Line ratios involving transitions in the ultraviolet (UV) and extreme-ultraviolet (EUV) regions of the spectrum frequently provide excellent temperature and density diagnostics for the emitting or absorbing plasmas. Over the past twenty five years or so, many such diagnostics have been developed for application to astronomical spectra, such as those of the solar transition region/corona and stellar observations from balloon, rocket and satellite-borne experiments (cf., Dwivedi 1994; Mason and Monsignori Fossi 1994). High-quality EUV data obtained from the spacecraft SOHO, provide the motivation for diagnostic applications to the analysis and interpretation of such data.

The usual procedure has been to look for line intensity ratios which are sensitive either to electron density N_e or electron temperature T_e . In various investigations it has been noticed that electron pressure within the chromosphere-corona transition region, and the corona, is either constant or varies slowly with height in the transition region and to some extent in the corona. The observed intensity of a particular line is due to several emitting layers. Each layer would have different electron density and temperature values but electron pressure would be nearly the same in all the emitting layers. The comparison of theoretical ratios with the observed values would then give the effective values of electron density and temperature within the emission regions.

It is, therefore, physically meaningful to study the variation of intensity ratios with electron density (and thus temperature) at constant pressure. This approach has been applied for spectroscopic diagnostics of several solar ions including NeV/MgV and SiVII/MgVII (cf., Dwivedi, Mohan & Raju 1997 and references cited therein).

Under the conditions that obtain in the Sun, the line intensity ratios are thus clearly sensitive to variations in both the electron temperature and density. Hence, in principle, they should only be used to determine N_e or T_e when the other plasma parameter has been independently estimated. In view of this, we investigate the problem from another standpoint. In what follows, we plot several ratio-ratio diagrams, such as log R_1 vs log R_2 and so on, for a grid of (log $N_{e,,}$ log T_e) values appropriate to the solar transition region. Using these figures it is possible to simultaneously determine both the electron temperature and density from the measured/computed values of the ratios. Such a technique has also been used by Keenan *et al.* (1995).

The ions NeV, MgV and SiVII, MgVII have their respective ionic concentrations maximum at about the same temperatures of 2.8×10^5 K and 6.3×10^5 K, respectively. Moreover, their ionization equilibrium curves overlap around the respective temperatures for maximum ionic concentrations. Therefore, these ionic pairs could be used for the electron density and temperature diagnostics of the relevant portions of the chromosphere-corona transition region and also to estimate their relative element abundances. We have computed theoretical line intensities for several NeV, MgV, SiVII and MgVII lines using a model solar atmosphere by Elzner (1976) and assuming values of 3.5×10^{-5}, 3.7×10^{-5} and 3.9×10^{-5} for the elemental abundances (relative to hydrogen) of Ne, Mg and Si, respectively (Meyer 1985). Theoretical intensities have been compared with the available observed quiet-Sun intensities for these lines. However, for want of data, we make use of these computed line intensities to deduce electron density and temperature from the ratio-ratio approach while emphasizing their applications with the SOHO data when available.

In section 2, we briefly describe the line emissivity. Atomic data are discussed in section 3. Observed and computed line intensities are considered in section 4. Electron density and temperature diagnostic aspects are examined in section 5. We make concluding remarks in the last section.

2. Line emissivity

The volume emission coefficient in a radiative transition from the upper level j to a lower level i for an optically thin spectral line is given by

$$\epsilon(\lambda_{ij}) = N_j A_{ji} \frac{hc}{4\pi\lambda_{ij}} \; (j > i) \; \mathrm{ergs\,cm^{-3}\,s^{-1}\,sr^{-1}} \tag{1}$$

where λ_{ij} is the wavelength for the transition $i \rightarrow j$, h is Planck's constant, c the velocity of light and A_{ji} is the spontaneous transition probability. The number density N_j of the emitting level of the ionic species can be parametrised as:

$$N_j(X^{+p}) = \frac{N_j(X^{+p})}{N(X^{+p})} \cdot \frac{N(X^{+p})}{N(X)} \cdot \frac{N(X)}{N(\mathrm{H})} \cdot \frac{N(\mathrm{H})}{N_e} \cdot N_e \tag{2}$$

where X^{+p} denotes the p^{th} ionization stage of the element X, $N_j(X^{+p})$ /$N(X^{+p})$ is the population of level j relative to the total population of the ion X^{+p}, $N(X^{+P})$ /$N(X)$ is

the ionization ratio of the ion X^{+p} . $N(X)$ /$N(H)$ is the abundance of the element X relative to hydrogen which may or may not be constant in the solar plasma. We have assumed $N(H)$ /N_e = 0.8 for the fully ionized plasma. The emissivity can now be expressed as:

$$\epsilon(\lambda_{ij}) = \frac{1.265 \times 10^{-9}}{\lambda_{ij}} \cdot A_{ji} \cdot \frac{N_j(X^{+p})}{N(X^{+p})} \cdot \frac{N(X^{+p})}{N(X)} \cdot \frac{N(X)}{N(\mathrm{H})} \cdot N_e. \tag{3}$$

We denote the line intensity as $I(\lambda_{ij})$ which is the intensity integrated over the line of sight. In the case of two lines emitted from the same ion, the intensity ratio can be expressed as

$$\frac{I(\lambda_{ij})}{I(\lambda_{kl})} = \frac{A_{ji}}{A_{lk}} \frac{\lambda_{kl}}{\lambda_{ij}} \frac{N_j(X^{+p})}{N_l(X^{+p})}. \tag{4}$$

The intensity ratio for the lines emitted from the same volume element but from different elements X and Y is then given by:

$$R = \frac{I(\lambda_{ij})}{I(\lambda_{kl})} = \frac{A_{ji}}{A_{lk}} \cdot r(j,l,X,Y) \cdot s(X,Y) \cdot N(X,Y) \tag{5}$$

Where

$$r(j,l,X,Y) = \frac{N_j(X^{+p})}{N(X^{+p})} \Big/ \frac{N_l(Y^{+q})}{N(Y^{+q})},$$

$$s(X,Y) = \frac{N(X^{+p})}{N(X)} \Big/ \frac{N(Y^{+q})}{N(Y)},$$

and

$$N(X,Y) = \frac{N(X)}{N(\mathrm{H})} \Big/ \frac{N(Y)}{N(\mathrm{H})}.$$

In the second case the intensity ratio depends on the relative ionic concentrations of the elements and their relative element abundances. The ionization equilibrium curves for NeV, MgV and SiVII, MgVII overlap around their respective temperatures for maximum ionic concentrations, respectively. We, therefore, assume that lines from NeV-MgV originate from the same emitting layers; similarly for the SiVII-MgVII ions. This assumption then justifies the use of equation (5) for line intensity ratios. We have solved the steady state equations for the various atomic levels to obtain N_j(NeV)/ N(NeV), N_j(MgV)/N(MgV), N_j(SiVII)/N(SiVII) and N_j(MgVII)/N(MgVII) as a function of electron density and temperature. We have considered the first 15 atomic levels for NeV, MgVII and the first 9 atomic levels for MgV, SiVII ions.

3. Atomic data

The atomic data needed to compute line intensities are the following: (**i**) wavelengths, (**ii**) radiative transition probabilities, and (**iii**) collision strengths. The wavelengths have been taken from Kelly & Palumbo (1973). The wavelengths for a few transitions which are not listed by Kelly & Palumbo have been estimated from the term values

Table 1. Line intensities of Ne V lines (N (Ne) / N (H) = 3.5 ×10^{-5}).

Transition $2s2p^3 \rightarrow 2s^22p^2$	Wavelength (Å)	Intensities (ergs cm^{-2} s^{-1} sr^{-1})	
		Computed (Vernazza & Reeves 1978)	Observed
$^3S^0_1 - {}^3P_0$	357.95	0.77	–
$^3S^0_1 - {}^3P_1$	358.48	2.32	–
$^3S^0_1 - {}^3P_2$	359.39	3.87	102.16
$^1P^0_1 - {}^1D_2$	365.61	2.73	136.11
$^1D^0_2 - {}^1D_2$	416.20	5.67	33.73
$^1P^0_1 - {}^1S_0$	416.82	0.62	–
$^3P^0_1 - {}^3P_0$	480.41	0.95	4.83
$^3P^0_0 - {}^3P_1$	481.28	1.02	–
$^3P^0_1 - {}^3P_1$	481.36	0.76	–
$^3P^0_2 - {}^3P_1$	481.37	1.15	–
$^3P^0_1 - {}^3P_2$	482.98	1.16	6.18
$^3P^0_2 - {}^3P_2$	482.99	3.66	–
$^3D^0_1 - {}^3P_0$	568.42	1.22	–
$^3D^0_1 - {}^3P_1$	569.76	0.85	–
$^3D^0_2 - {}^3P_1$	569.83	2.75	–
$^3D^0_2 - {}^3P_2$	572.11	0.80	8.76
$^3D^0_3 - {}^3P_2$	572.34	4.84	–
$^5S^0_2 - {}^3P_1$	1137.0	0.28	–
$^5S^0_2 - {}^3P_2$	1146.1	0.70	–

Table 2. Line intensities of Mg V lines (N (Mg) / N (H) = 3.7 × 10^{-5}).

Transition $2s2p^5 \rightarrow 2s^22p^4$	Wavelength (Å)	Intensities (ergs cm^{-2} s^{-1} sr^{-1})	
		Computed (Vernazza & Reeves 1978)	Observed
$^1P^0_1 - {}^1D_2$	276.58	2.87	–
$^3P^0_1 - {}^3P_2$	351.09	1.61	–
$^3P^0_0 - {}^3P_1$	352.20	1.45	–
$^3P^0_2 - {}^3P_2$	353.09	5.52	100
$^3P^0_1 - {}^3P_1$	353.30	0.97	–
$^3P^0_1 - {}^3P_0$	354.22	1.28	–
$^3P^0_2 - {}^3P_1$	355.33	1.73	–
$2s^22p^4 \rightarrow 2s^22p^4$			
$^1S_0 - {}^3P_1$	1324.43	0.19	–
$^1D_2 - {}^3P_2$	2783.34	0.13	–

given by Edlén (1982). For NeV and MgVII the various transition probabilities have been taken from Nussbaumer and Rusca (1979) and Aggarwal (1986). Transition probabilities for the SiVII ion have been taken from Bhatia, Feldman & Doschek

Table 3. Line intensities of Mg VII lines (N (Mg) / N (H) = 3.7×10^{-5}).

Transition	Wavelength	Intensities (ergs cm^{-2} s^{-1} sr^{-1})	
$2s2p^3 \rightarrow 2s^22p^2$	(Å)	Computed	Observed
$^3S_1^0 - {}^3P_0$	276.15	2.46	2.93[a]
$^3S_1^0 - {}^3P_1$	276.99	7.37	23.41[a] (blended)
$^3S_1^0 - {}^3P_2$	278.41	12.38	17.56[a]
$^1P_1^0 - {}^1D_2$	280.74	2.53	
$^1D_2^0 - {}^1D_2$	319.02	5.79	
$^1P_1^0 - {}^1S_0$	320.50	0.59	
$^3P_1^0 - {}^3P_0$	363.75	2.45	
$^3P_0^0 - {}^3P_1$	365.17	2.60	
$^3P_1^0 - {}^3P_1$	365.21	2.88	136.11[b] (blended)
$^3P_2^0 - {}^3P_1$	365.23	2.09	
$^3P_1^0 - {}^3P_2$	367.64	9.77	655[b] (blended by Mg^{+8})
$^3P_2^0 - {}^3P_2$	367.68	2.93	
$^3D_1^0 - {}^3P_0$	429.13	2.89	
$^3D_1^0 - {}^3P_1$	431.17	1.88	38.22[b] (blended by Mg^{+7})
$^3D_2^0 - {}^3P_1$	431.32	6.69	
$^3D_2^0 - {}^3P_2$	434.71	1.70	28.32[b] (blended by Ne^{+5})
$^3D_3^0 - {}^3P_2$	434.92	11.42	
$^5S_2^0 - {}^3P_1$	854.70	0.40	
$^5S_2^0 - {}^3P_2$	868.13	0.95	
$2s^22p^2 \rightarrow 2s^22p^2$			
$^1S_0 - {}^3P_1$	1189.82	0.54	–
$^1D_2 - {}^3P_2$	2629.00	0.63	–

[a] Malinovsky & Heroux (1973).
[b] Vernazza & Reeves (1978).

Table 4. Line intensities of SiVII lines (N (Si) / N (H) = 3.9×10^{-5}).

Transition	Wavelength	Intensities (ergs cm^{-2} s^{-1} sr^{-1})	
$2s2p^5 \rightarrow 2s^22p^4$	(Å)	Computed	Observed
$^1P_1^0 - {}^1D_2$	217.83	1.78	–
$^3P_1^0 - {}^3P_2$	272.64	6.0	5.12[a]
$^3P_0^0 - {}^3P_1$	274.17	3.74	–
$^3P_2^0 - {}^3P_2$	275.35	22.39	14.63[a]
$^3P_1^0 - {}^3P_1$	275.67	3.46	2.19[a]
$^3P_1^0 - {}^3P_0$	276.84	4.52	3.66[a]
$^3P_2^0 - {}^3P_1$	278.45	7.14	–
$2s^22p^4 \rightarrow 2s^22p^4$			
$^1S_0 - {}^3P_1$	1049.15	0.40	–
$^1D_2 - {}^3P_2$	2147.35	1.03	–

[a] Malinovsky & Heroux (1973).

(1979). In the case of MgV ion, for a given transition logarithmic value of transition probabilities of SiVII, SIX and ArXI (Bhatia, Feldman & Doschek 1979) were plotted against the inverse atomic number. A linear fit between log A_{ji} and $1/Z$

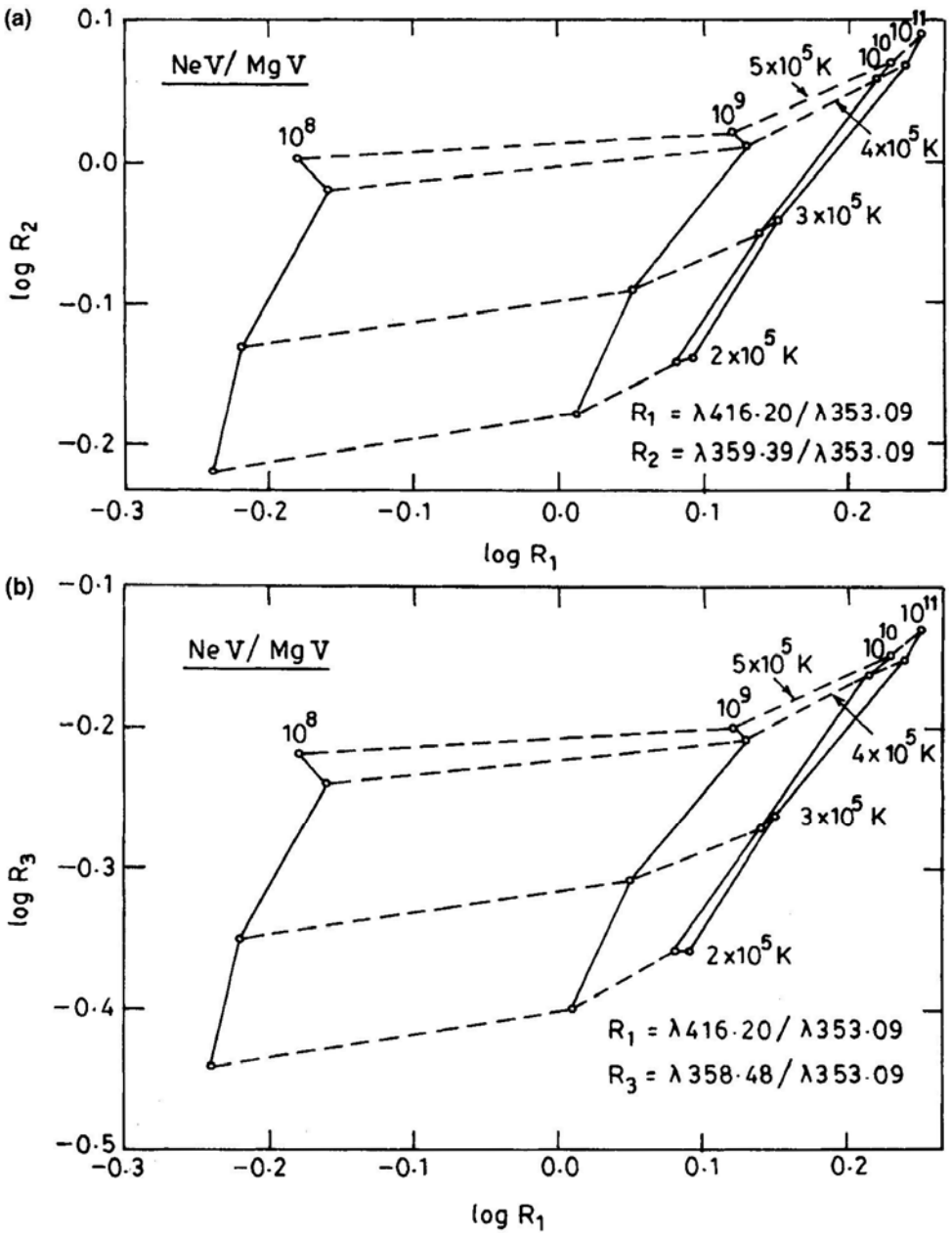

Figure 1. (**a**) Plot of the theoretical NeV/MgV emission line ratio log R_1 = λ416.20/ λ353.09 against log R_2 = λ359.39/λ353.09 for a range of electron temperatures (log T_e = 5.3–5.7; T_e in K) and electron densities (logN_e = 8–11, N_e in cm^{-3}). Points of constant T_e are connected by dashed lines, while those of constant N_e are joined by solid lines; (**b**) Same as Fig. l(a) except for log R_1=λ416.20/λ353.09 against log R_3 =λ 358.48/λ353.09.

(Z being the atomic number) was found to be valid for all the transitions. The respective A_{ji} values for MgV transitions were thus obtained.

The various collision strengths required to solve the steady state equations for the atomic levels have been expressed in terms of effective collision strengths. Collision strengths are in general a function of the incident electron energy. The integral of the collision strength over the incident electron energies gives us the effective collision strength. In simple cases it is possible to get an analytical form for the effective

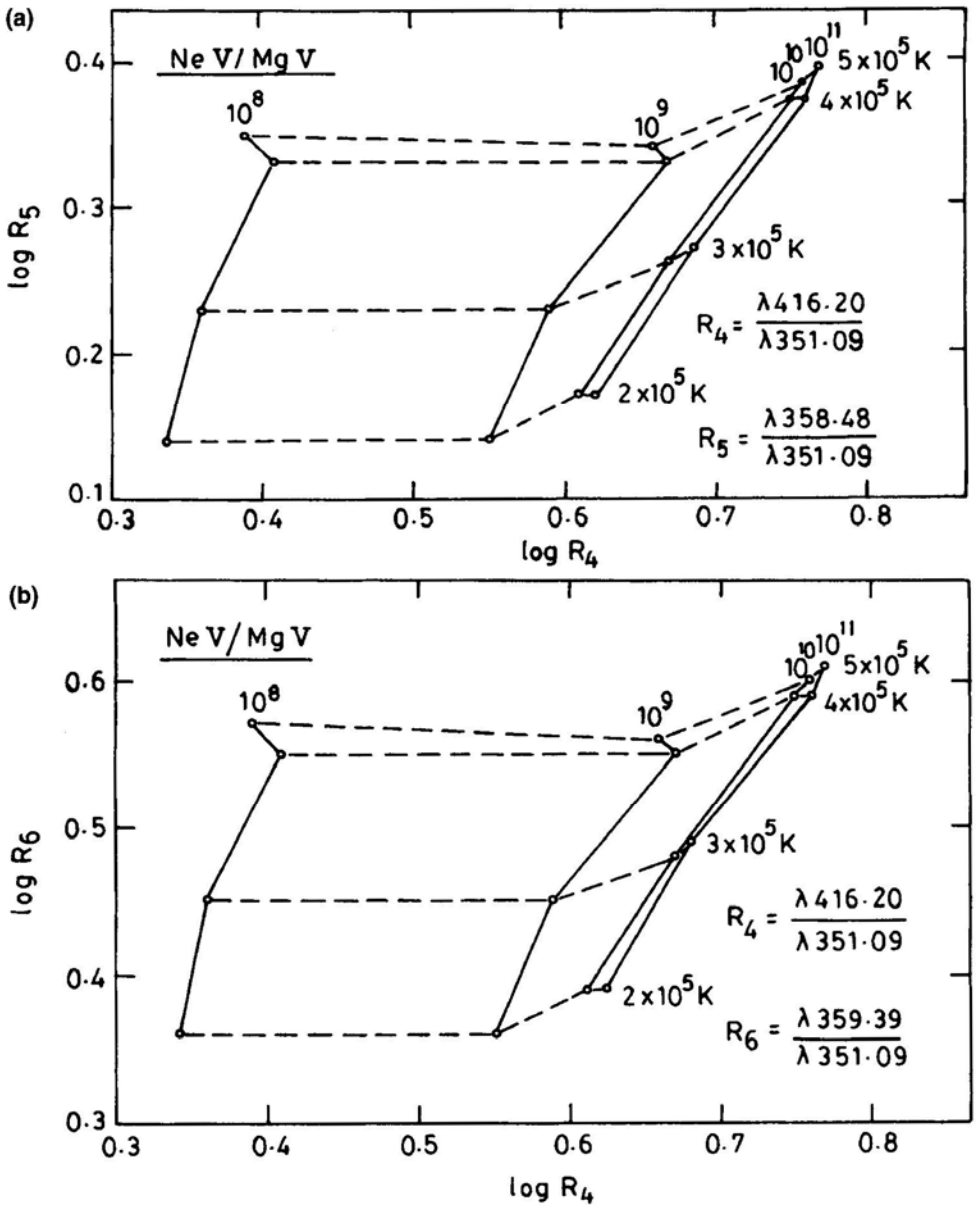

Figure 2 (**a**) same as Fig. 1 except for log R_4 = λ416.20/ 351.09 against log R_5 = λ358.48/λ351.09; (**b**) log R_4 =λ416.20/λ351.09 against log R_6 =λ359.39/λ351.09.

collision strength. In such cases we get the effective collision strengths as a function of the electron temperature for which suitable analytical forms have been derived. Thus we have obtained effective collision strengths for NeV, MgV, SiVII and MgVII ions for the various transitions as a function of electron temperature using the following sources : Aggarwal (1984,1985,1986) for NeV and MgVII ions; and Bhatia, Feldman & Doschek (1979) for MgV and SiVII ions.

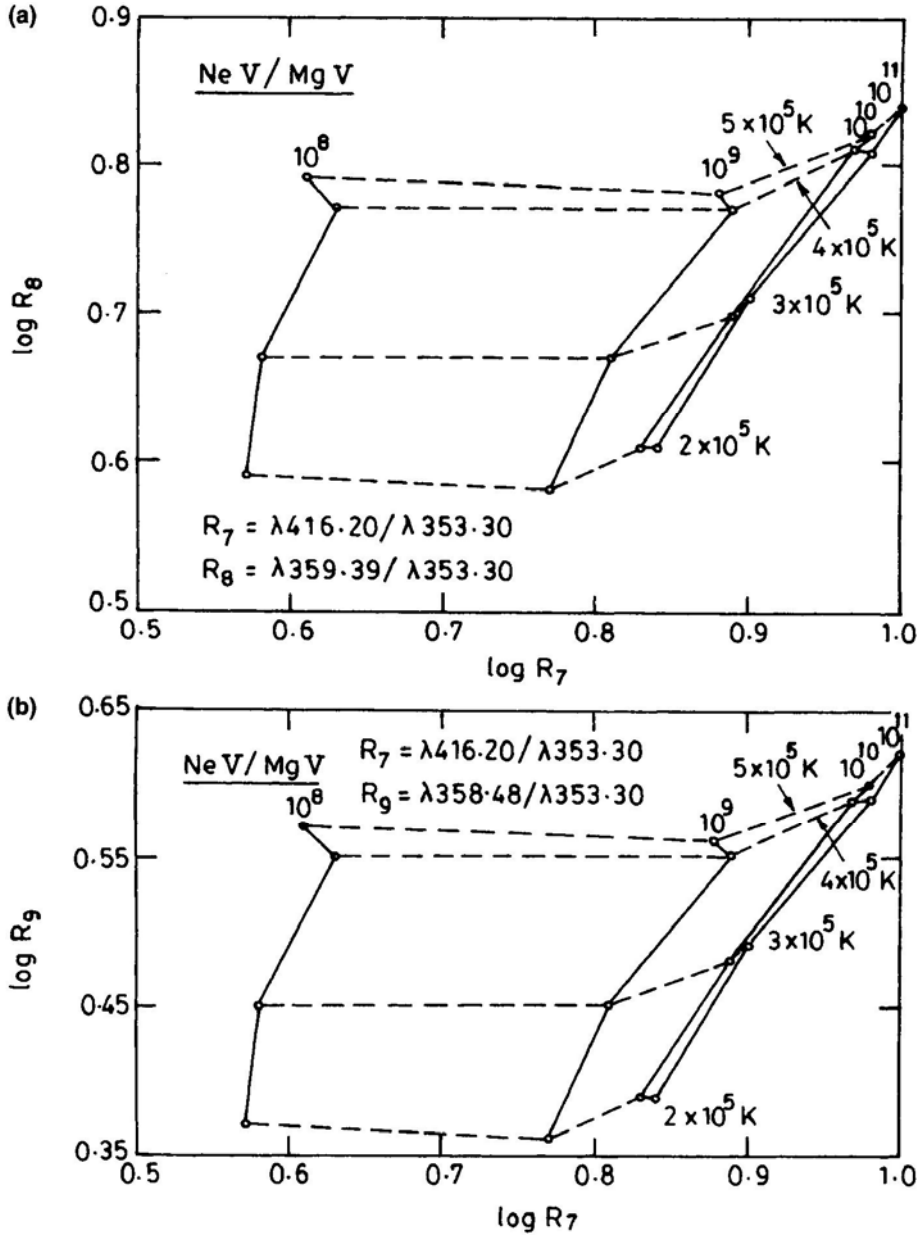

Figure 3. (**a**) Same as Fig. 1 except for log R_7 =λ416.20/λ353.30 against log R_8 = λ359.39/λ353.30; (**b**) logR_7 = λ416.20/λ353.30 against log R_9 = λ358.48/λ353.30.

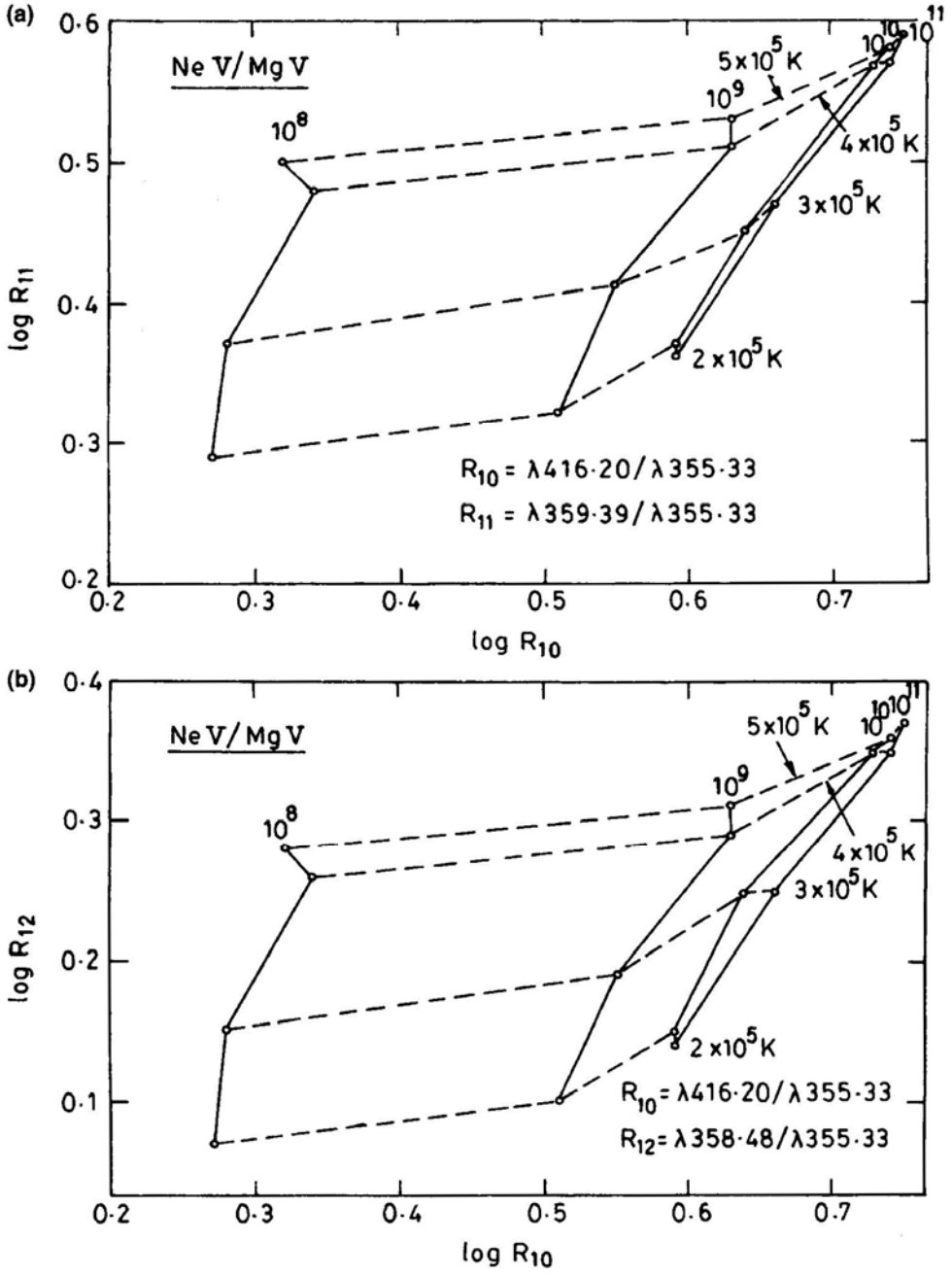

Figure 4 (**a**) Same as Fig 1 except for log R_{10} = λ416.20/λ355.33 against log R_{11} = λ359.39/λ355.33; (**b**) log R_{10} =λ416.20/λ355.33 against log R_{12}= 358.48/ 355.33.

4. Observed and theoretical intensities

Theoretical line intensities have been computed assuming: (**i**) spherically symmetric quiet-Sun model-atmosphere (Elzner 1976), (**ii**) ionic concentrations tabulated by

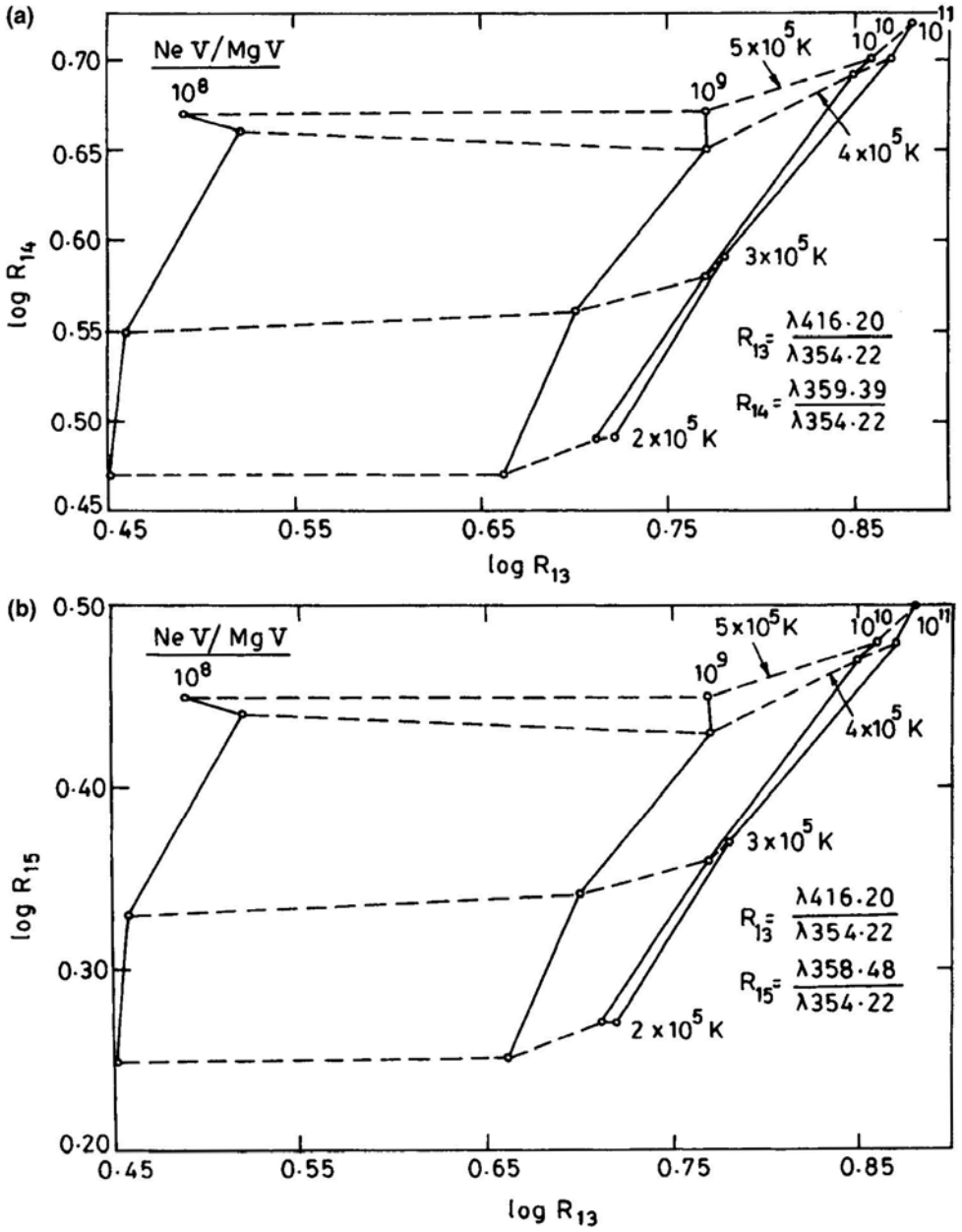

Figure 5. (**a**) Same as fig 1 except for log R_{13} = λ416.20/λ354.22 against log R_{14} = λ359.39/λ354.22; (**b**) log R_{13} =λ416.20/λ354.22 against log R_{15} =λ358.48/λ354.22.

Arnaud & Rothenflug (1985), and (**iii**) values of 3.5×10^{-5}, 3.7×10^{-5} and 3.9×10^{-5} for the element abundance (relative to hydrogen) of Ne, Mg and Si, respectively (Meyer 1985). In Tables 1 to 4 we have listed the theoretical and available observed line intensities for the ions NeV, MgV, SiVII and MgVII. To resolve the discrepancies between the computed and observed intensities, observations at high spectral resolutions with a more sensitive spectral scan are needed. Moreover, the solar atmosphere is completely

Table 5. NeV/MgV electron densities and temperatures (N_e , T_e) derived from ratio-ratio diagrms (cf., Figs. 1 to 5).

Ratio-ratio	N_e (cm^{-3})	T_e (K)
(R_1, R_2)	8.4×10^8	2.4×10^5
(R_1, R_3)	8.5×10^8	2.3×10^5
(R_4, R_5)	8.6×10^8	2.2×10^5
(R_4, R_6)	8.7×10^8	2.2×10^5
(R_7, R_8)	8.6×10^8	2.2×10^5
(R_7, R_9)	8.6×10^8	2.2×10^5
(R_{10}, R_{11})	8.6×10^8	2.4×10^5
(R_{10}, R_{12})	8.6×10^8	2.4×10^5
(R_{13}, R_{14})	8.2×10^8	2.1×10^5
(R_{13}, R_{15})	8.2×10^8	2.1×10^5

Table 6. SiVII/MgVII electron densities and temperatures (N_e, T_e) derived from ratio-ratio diagrams (cf., Figs. 6 to 9).

Ratio-ratio	N_e (cm^{-3})	T_e (K)
(R_1, R_2)	8.1×10^8	6.2×10^5
(R_3, R_2)	8.0×10^8	6.2×10^5
(R_4, R_2)	8.5×10^8	6.2×10^5
(R_5, R_6)	8.3×10^8	6.0×10^5

inhomogeneous and the computed intensity values based on a spherically symmetric model can at best serve as an indicator of the feasibility of observing these lines.

5. Density and temperature diagnostic NeV/MgV line ratios

We show in Figs. 1 to 5 line diagnostics for NeV/MgV ions in the form of ratio-ratio diagrams. The line intensity ratios are dependent, in addition, on the relative element abundances and relative ionic concentrations of NeV and MgV. The ratio-ratio curves in these figures are drawn for equal element abundances of Ne and Mg, which means these line ratio curves are the normalized values given by the expressions

$$\{I(\lambda(\mathrm{NeV}))/I(\lambda(\mathrm{MgV}))\}^{\mathrm{normalized}} = \{I(\lambda(\mathrm{NeV}))/I(\lambda(\mathrm{MgV}))\}^{\mathrm{actual}} \Big/ \left\{ \left(\frac{N(\mathrm{Ne})}{N(\mathrm{H})}\right) \Big/ \left(\frac{N(\mathrm{Mg})}{N(\mathrm{H})}\right) \right\}. \quad (6)$$

Making use of the computed line intensities, we derive N_e and T_e from the ratio-ratio diagrams. These are listed in Tables 5–6. A consistent value of about 8×10^8 cm^{-3} for the density and 2×10^5 K for the temperature are obtained from the NeV/MgV ratio-ratio diagrams (cf., Table 5). It should, however, be noted that abundance anomaly must be taken account of in the analysis and interpretation of observations. These diagrams will be very useful in analysing and interpreting data from the CDS spectrometer when available. Also, we can use these diagrams to deduce N_e and T_e simultaneously from the observed line intensity ratios.

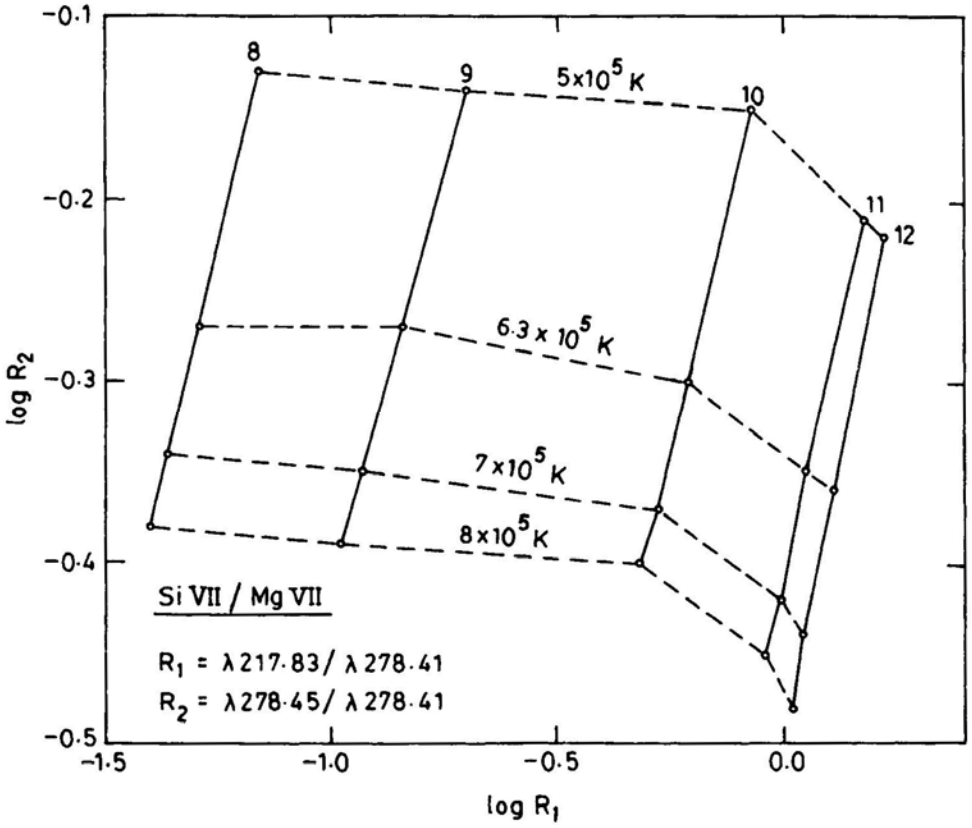

Figure 6. Plot of the theoretical SiVII/MgVII emission line ratio log R_1=λ21.83/ λ278.41 against log R_2 = λ278.45/λ278.41 for a range of logarithmic electron temperatures (log T_e = 5.7–5.9; T_e in K) and logarithmic electron densities (log N_e = 8–11; N_e in cm^{-3}). Points of constant T_e are connected by dashed lines, while those of constant N_e are joined by solid lines.

5.1 *SiVII /MgVII line ratios*

We show in Figs. 6 to 9 line diagnostic ratio-ratio diagrams for SiVII/MgVII The derived values for N_e and T_e are given in Table 6. A consistent value of about 8×10^8 cm^{-3} for density and 6×10^5 K for temperature is obtained. The constant electron pressure of about 5×10^{14}cm^{-3} K is consistent with the transition region solar plasma. The current observations from the CDS/SOHO will be meaningfully used to deduce N_e and T_e from these ratio-ratio diagrams. This will also greatly help in the analysis and interpretation of high-quality EUV data from the CDS spectrometer.

6. Concluding remarks

Simultaneous evaluation of the plasma temperature and the density through the line intensity ratio-ratio diagrams seem to be an excellent diagnostic technique for inhomogeneous solar atmosphere. Although we have used theoretical line intensities based on an unrealistic solar model to deduce N_e and T_e, the ratio-ratio diagrams

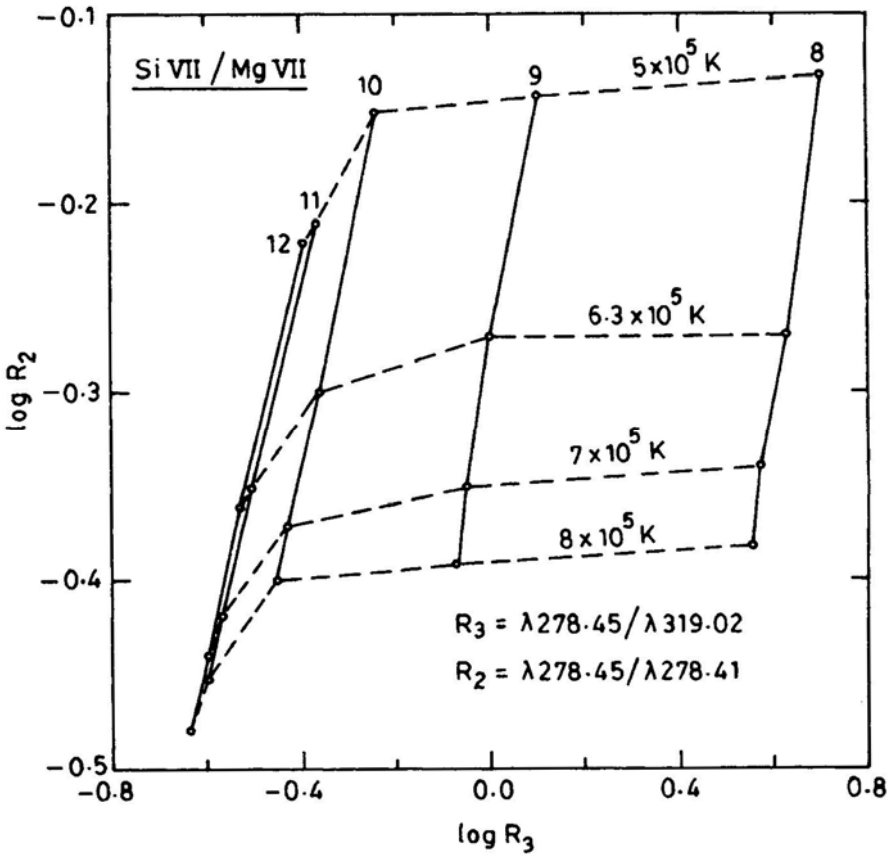

Figure 7. Same as Fig. 6 except for log R_4 =λ278.45/λ319.02 against log R_2 =λ278.45/ λ278.41.

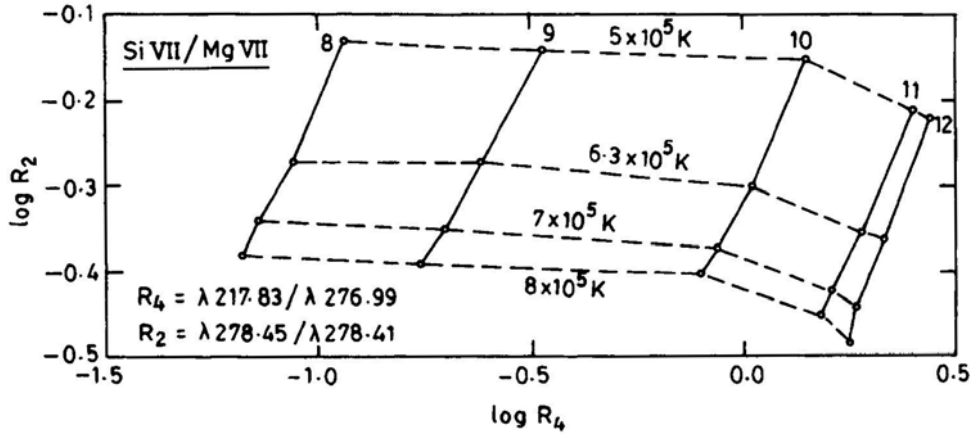

Figure 8. Same as Fig. 6 except for log R_4 = λ217.83/λ276.99 against log R_2 = λ 278.45/ λ278.41.

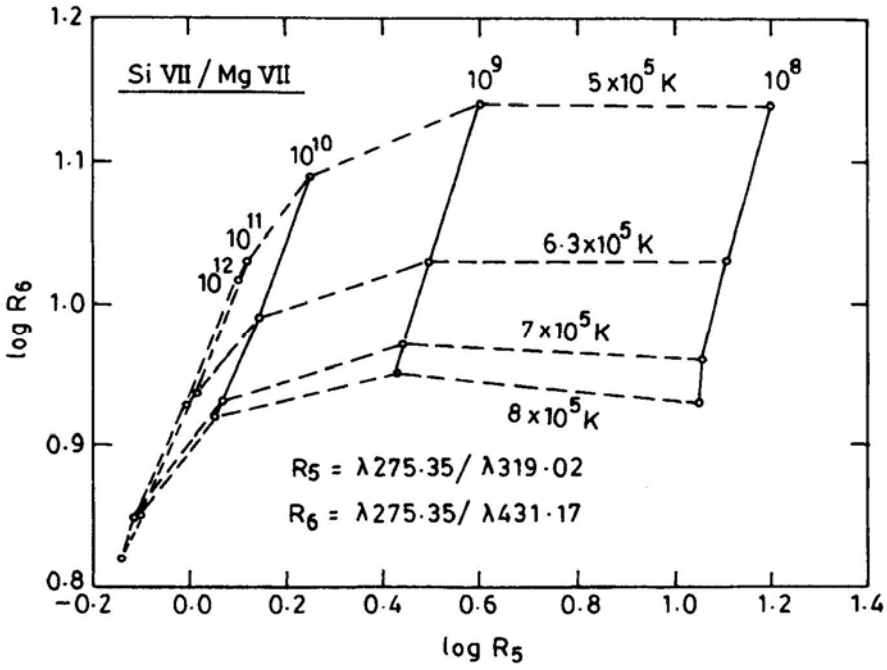

Figure 9. Same as Fig. 6 except for log R_5 =λ275.35/λ319.02 against log R_6 =λ275.35/ λ431.17.

presented in this paper can always be applied, making use of the observed line intensities. Such observations are expected from the high-quality EUV data from CDS/SOHO. While we have shown NeV/MgV and SiVII/MgVII lines to be potentially useful for diagnostics, we expect to estimate Ne/Mg and Si/Mg relative element abundances and their possible variation in different solar structures when such data become available from CDS/SOHO.

Acknowledgements

This work was enabled by the financial support to Anita Mohan from the Department of Science and Technology, New Delhi under the SERC Young Scientist Programme. We wish to thank the Editor for critical reading of the paper.

References

Aggarwal, K. M. 1984, *Astrophys. J. Suppl.*, **56,** 303.
Aggarwal, K. M. 1985, *Astrophys. J. Suppl,* **58,** 289.
Aggarwal, K. M. 1986, *Astrophys. J. Suppl.*, **61,** 699.
Arnaud, M., Rothenflug, R.1985, *Astr. Astrophys. Suppl.*, **60,** 425.
Bhatia, A. K., Feldman, U., Doschek, G.1979, *Astr. Astrophys.*,**80.** 22.
Dwivedi, B. N.1994, *Space Sci. Rev.*, **65,** 289.
Dwivedi, B. N., Mohan, A, Raju, P. K. 1997, *Adv. Space Res.*, **20,** 12, 2271.
Edlén, B. 1982, *Phys. Scripta*, **26**, 71.

Elzner, L. R. 1976, *Astr.Astrophys.*, **47,** 9.
Kelly, R. L., Palumbo, L. J. 1973, Atomic and Ionic Emission Lines below 2000 Å, NRL Report 7599.
Keenan, F. P., Foster, V. J., Reid, R. H. G., Doyle, J. G., Zhang, H. L., Pradhan, A. K. 1995, *Astr. Astrophys.*, **300,** 534.
Malinovsky, M., Heroux, L. 1973, *Astrophys. J.*, **181,** 1009.
Mason, H. E., Monsignori Fossi, B. C. 1994, *Astr. Astrophys. Rev.*, **6,** 123.
Meyer, J. P. 1985, *Astrophys. J. Suppl.*, **57,** 151.
Nussbaumer, H., Rusca, C. 1979, *Astr. Astrophys.* **72,** 129.
Vernazza, J. E., Reeves, E. M. 1978, *Astrophys. J. Suppl*, **37**, 485.